Supporting information

Spray coating thin films on three-dimensional surfaces for a semi-transparent capacitive touch device

Tian Carey[1], Chris Jones[2], Fred Le Moal[2], Davide Deganello[3] and Felice Torrisi*[1]

[1] *Cambridge Graphene Centre, Cambridge University, Cambridge, CB3 0FA, UK*

[2] *Novalia Ltd, Impington, Cambridge, CB24 9N, UK*

[3] *Welsh Centre for Printing and Coating, College of Engineering, Swansea University, Swansea, SA1 8EN, UK*

1.0 Optical Absorption Spectroscopy of Inks

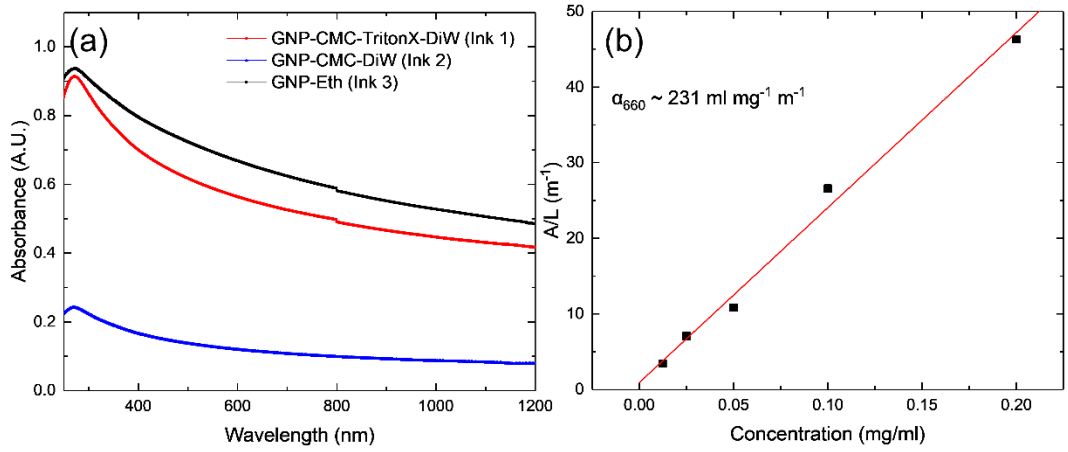

Figure S1: (a) Absorption spectra for ink 1,2 and 3 which are diluted to a 1:20 ratio (ink 1 and 2) and 1:100 (Ink 3), to avoid possible scattering losses at higher concentrations. (b) The optical absorbance (λ = 660nm) divided by the cell length (1 cm) is plotted as a function of the PEDOT:PSS concentration in ethanol solutions.

Optical Absorption Spectroscopy (OAS) is used to estimate the inks concentration of GNP[1,2] (Fig. S1a) after centrifugation via the Beer-Lambert law according to the relation A = α cl, where A is the absorbance, l [m] is the light path length, c [g/L] is the concentration of dispersed graphitic material, and α [L g^{-1} m^{-1}] is the absorption coefficient. By measuring the absorption (λ = 660 nm) in a UV-Vis-NIR spectra (Figure 1(a)) (Agilent Cary 7000 UMS) the concentration of the inks GNP-CMC-TritonX-DiW, (Ink 1, 0.8 mg/ml), GNP-CMC-DiW (Ink 2, 0.12mg/ml) and GNP-Eth (Ink 3, 2.6mg/ml) can be extracted using α ~1390 ml mg^{-1} m^{-1} [1] for GNP-CMC-TritonX-DiW (ink 1) and GNP-CMC-DiW (ink 2) and α ~2460 ml mg^{-1} m^{-1} [2] for GNP-Eth (ink 3).

To determine the absorption coefficient of PEDOT:PSS, the optical absorbance (λ = 660nm) divided by the cell length (1 cm) is plotted as a function of the PEDOT:PSS concentration in ethanol solutions in figure S1b. The concentration is calculated from the dilution of a commercial PEDOT:PSS solution (Sigma-Aldrich 739316, 0.8 w/v). A linear fit of the dataset determines an absorption coefficient of α ~231 ml mg^{-1} m^{-1}

1.1 Characterisation of Inks

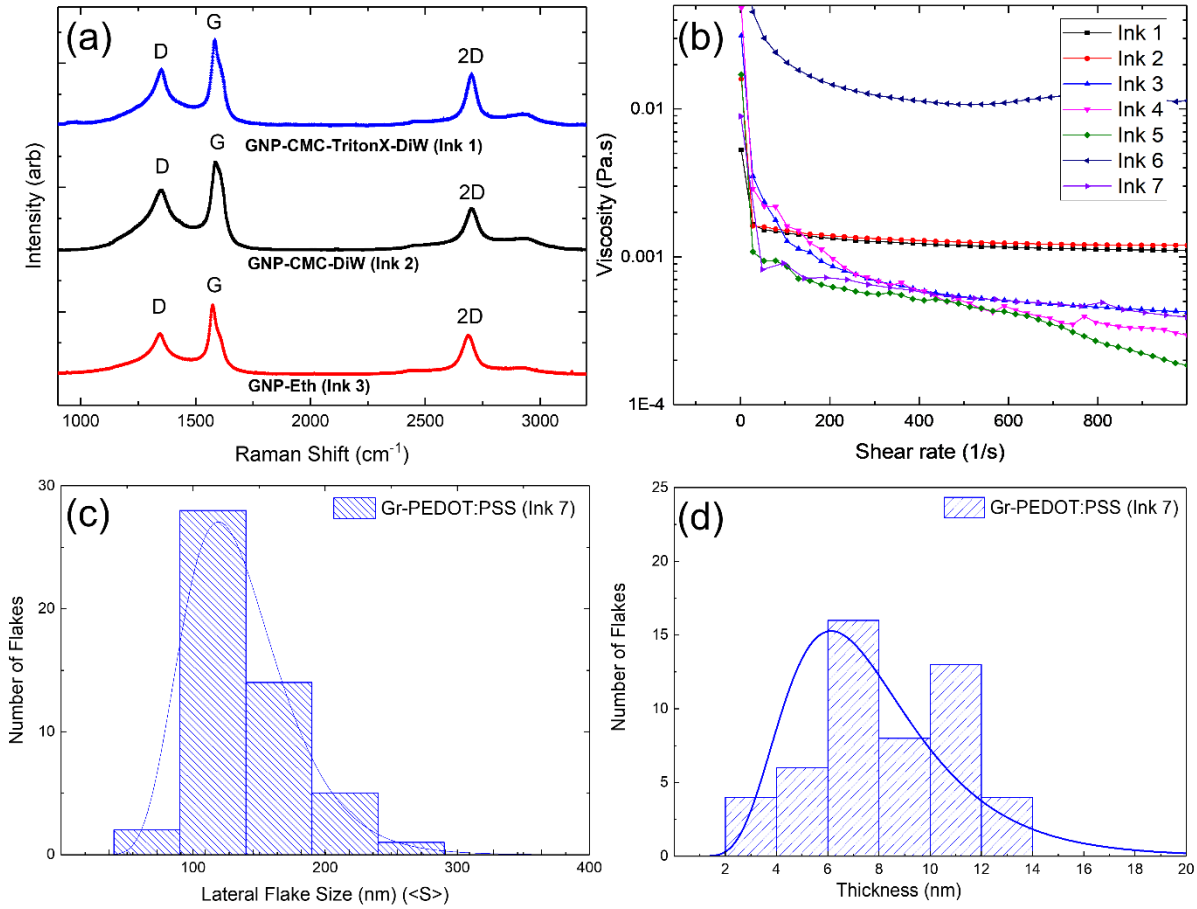

Figure S2: (a) Raman spectra acquired at 514.5nm for Ink 1, 2 and 3. (b) The viscosity of ink 1-7 as a function of shear rate. (c) The lateral size and (d) thickness of 50 graphene flakes in ink 7.

Figure S2a shows Raman spectra acquired at 514.5nm for drop casted films of ink 1-3 on a SiO_2/Si substrate. Each spectra for Ink 1-3 shows the typical G, D and single lorentzian fit of the 2D peak which is typical for graphene as described in the main text. Moreover the Disp(G) ~ 0.09 cm^{-1} nm^{-1} indicate that the defects associated with the D peak are mostly attributed to the edges of the flakes[3]. Figure S2b shows the viscosity as a function of shear rate for each inks 1-7, which is measured using a parallel plate rotational rheometer (DHR rheometer TA instruments). Shear thinning is observed in all inks and the infinite-rate viscosity is found (table 1 main text). The lateral size $< S >$ and thickness of the graphene flakes in the inks (figure S2c and S2d) were estimated by atomic force microscopy (AFM) (Bruker Dimension Icon). AFM statistics of < S > (Fig. S2c), defined as $< S >= \sqrt{xy}$ where x and y are the length and width of the flake show a log-normal distribution[4] for the Gr-PEDOT:PSS flakes peaked at 117nm. In Figure S2d the Gr-PEDOT:PSS flake thicknesses follow a log-normal distribution[4] which peaks at 6nm indicating that these are few layer graphene flakes.

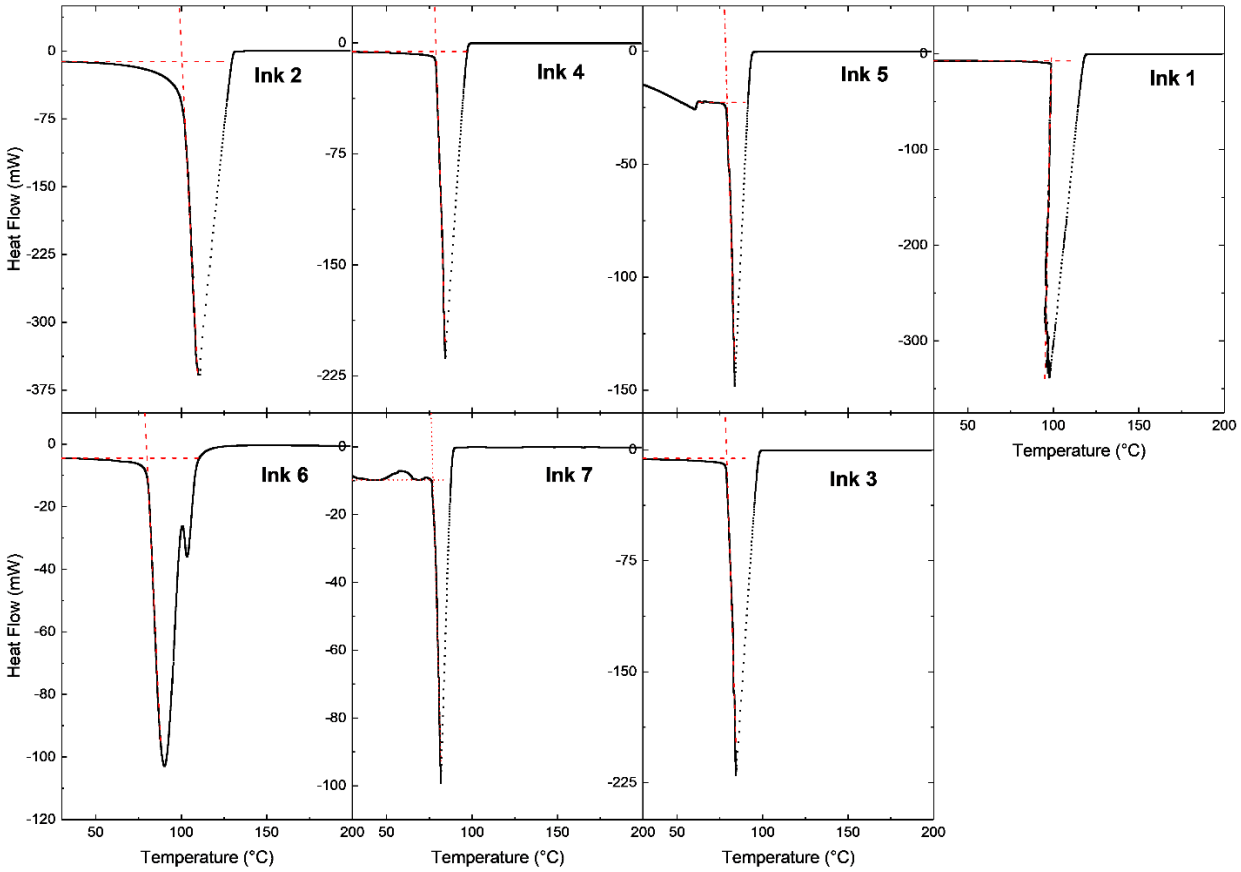

Figure S3: Differential Scanning Calorimetry is used to determine the boiling point of each ink 1-7.

In figure S3 the boiling points of each ink were determined using a Q20 DSC (TA instruments). Firstly ~10mg of ink is added to a pan which is then sealed with a hermetic pin hole lid (diameter 75 μm). Thermal profiles are taken from an initial temperature of 25°C which is then ramped at a rate of 5°C/min to 200°C. For each ink a line of best fit can be extruded from the baseline and at the endothermic phase transition so that the boiling point for each ink can be determined (values found in table 1 main text).

1.2 Surface energy of PET substrate

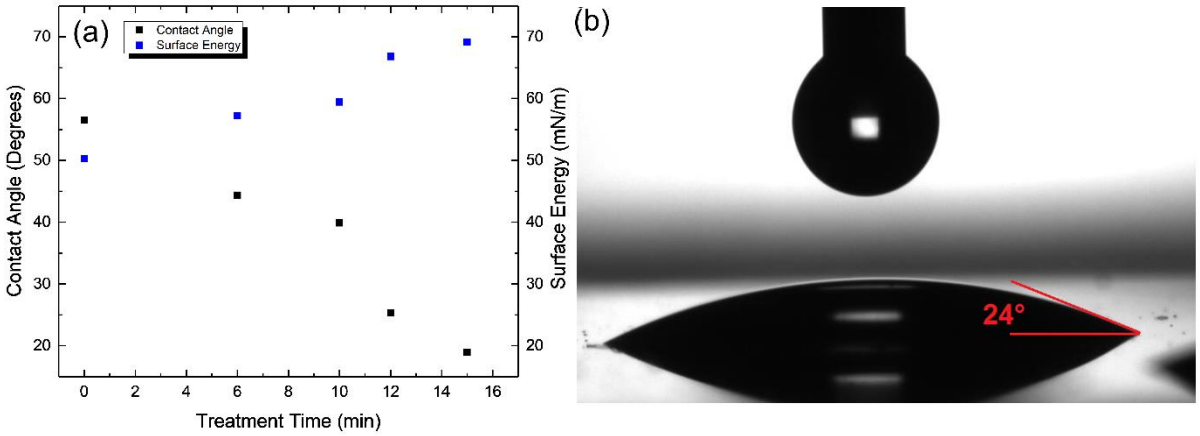

Figure S4: (a) Contact angle as a function of UV ozone treatment time (b) Contact angle at which a deionized water droplets meets a PET UV ozone treated (~12min) surface demonstrating an increase in surface energy.

Figure S4a plot the contact angle of a 1 µL of deionised water droplet onto a PET substrate (Hififilm PMX729) which has been treated by UV ozone system (Nano Bio Analytics UVC-1014) (4 W at 254 nm) for a series of treatment times up to 15min. It was found that the contact angle (θ_c) between the substrate and a tangent drawn to the liquid drop decreased from (~56°) to (~19°) following a linear relationship, indicating an increase in surface energy. The surface energy increase is calculated using Neumann's equation of state[5],

$$\gamma_{sl} = \gamma_{lv} + \gamma_{sv} - 2\sqrt{\gamma_{lv}\gamma_{sv}}\, e^{-\beta(\gamma_{lv}-\gamma_{sv})^2} \quad (1)$$

And when combined with Young's equation,

$$\gamma_{sv} = \gamma_{sl} + \gamma_{lv}\cos\theta \quad (2)$$

Yields,

$$\cos\theta = -1 + 2\sqrt{\frac{\gamma_{sv}}{\gamma_{lv}}}\, e^{-\beta(\gamma_{lv}-\gamma_{sv})^2} \quad (3)$$

Where the interfacial tension between the liquid and solid is γ_{sl}, the surface energy of the solid is γ_{sv} and the surface tension of the liquid is γ_{lv}.[5] Using a value of β = 0.0001247

$(m^2/mJ)^2$ which is determined empirically[5] we find an initial PET surface energy of 50.3 mN/m and after 15min of UV ozone treatment the surface energy increases to 69.2 mN/m.

1.3 Characterisation Techniques for thin films

Several techniques are available to characterise film topography of a sprayed film[6]. Optical techniques have proven successful for determining the morphological uniformity in the past, Susanna et. al.[7] has used optical microscopy images to characterise the morphology of spray coated polymer blends. While Scardaci et. al.[8] has used SEM images and developed a FOM to indicate uniformity. Mechanical methods such as stylus profilometry and atomic force microscopy can be influenced by substrate roughness when the film thickness is of similar magnitude, therefore making the topography hard to resolve in the case of our PET substrate (Root mean square height roughness, S_q = 17.8nm). Moreover the aforementioned techniques are restricted to the investigation of areas that are a few millimetres wide and therefore do not give a good indication of the long range morphological uniformity. For larger areas (~cm's) water sensitive papers have been used which change colour when water droplets make contact, the cards can then be imaged with a camera and post processed with software. However they cannot be used with organic solvents, are sensitive to humidity and the morphology is dependent on the roughness and surface energy of the paper which requires calibration equations to be used to account for droplet spreading[9]. In order to characterise the morphological uniformity of our large area films we use a similar technique using a simple desktop scanner (HP Deskjet 3050A) (see methods in main text) to obtain images of our films followed by post processing in alignment to methods used for water sensitive papers. This allows use to characterise the morphological uniformity of films which have been sprayed with organic material while also allowing us to see the long range uniformity of the films directly on the PET substrate.

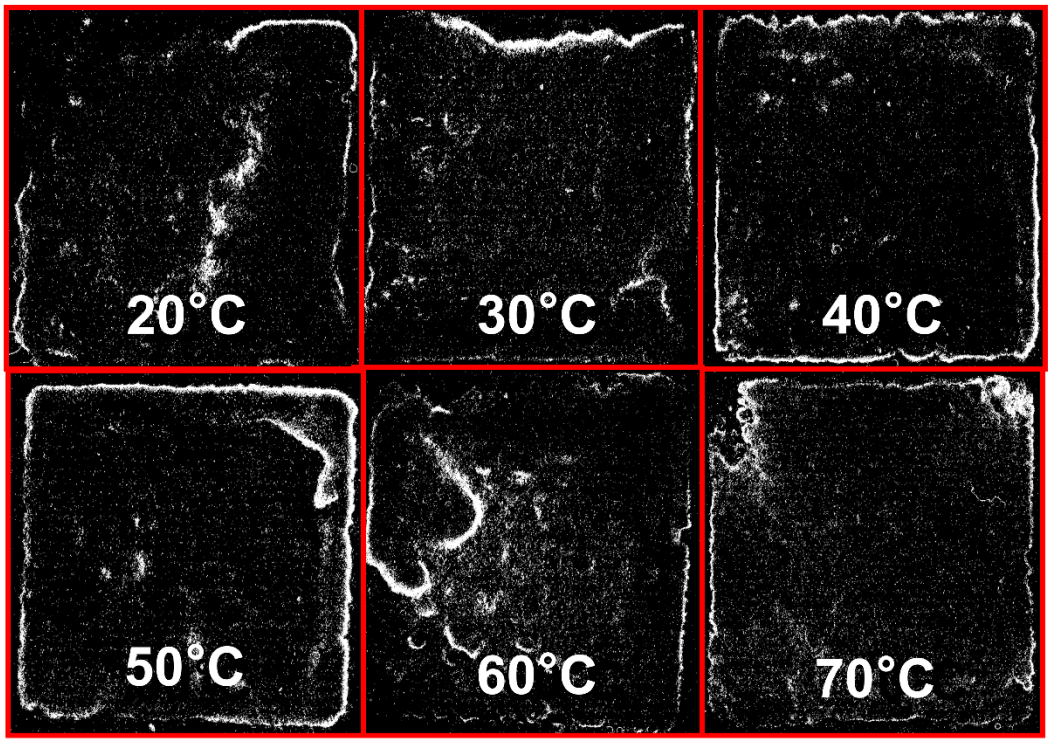

Figure S5: Morphology of a low surface tension (35 mN/m), high boiling point (99°C) ink (ink 1) as a function of temperature. Each box is 2.5cm by 2.5cm in length and width.

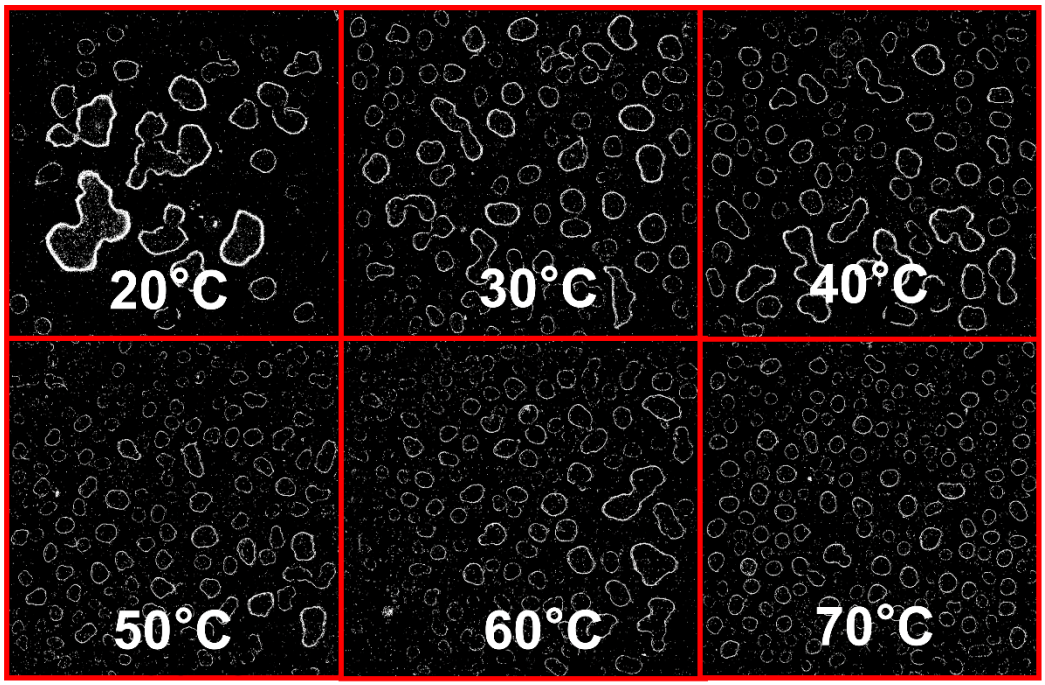

Figure S6: Morphology of a high surface tension (74 mN/m), high boiling point (100°C) ink (ink 2) as a function of temperature. Each box is 2.5cm by 2.5cm in length and width.

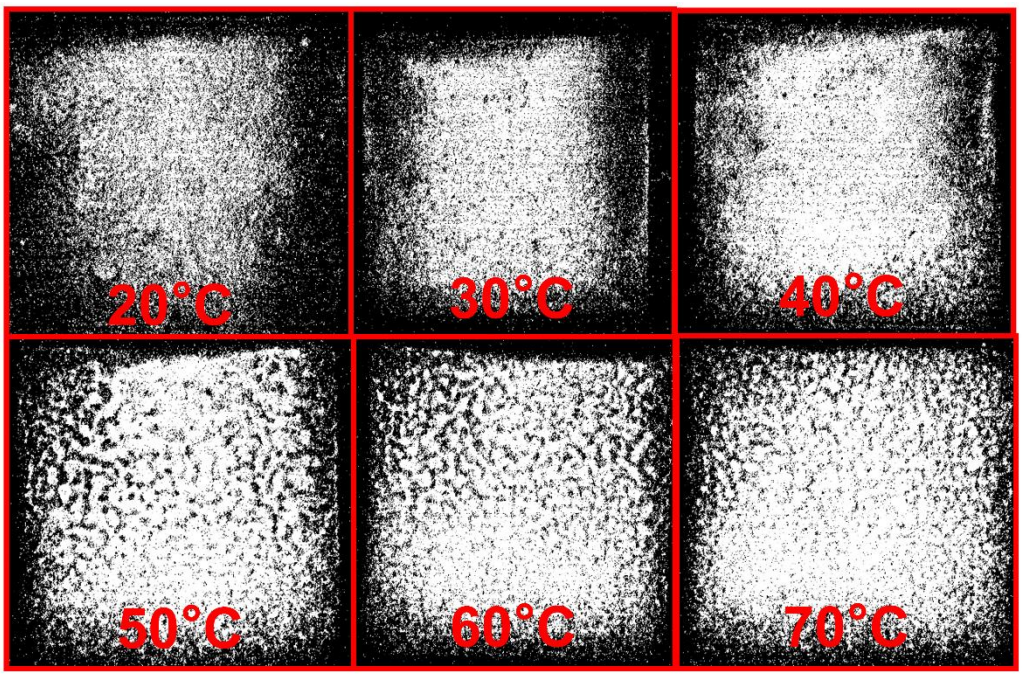

Figure S7: Morphology of a low surface tension (30 mN/m), low boiling point (79 °C) ink (ink 3) as a function of temperature. Each box is 2.5cm by 2.5cm in length and width.

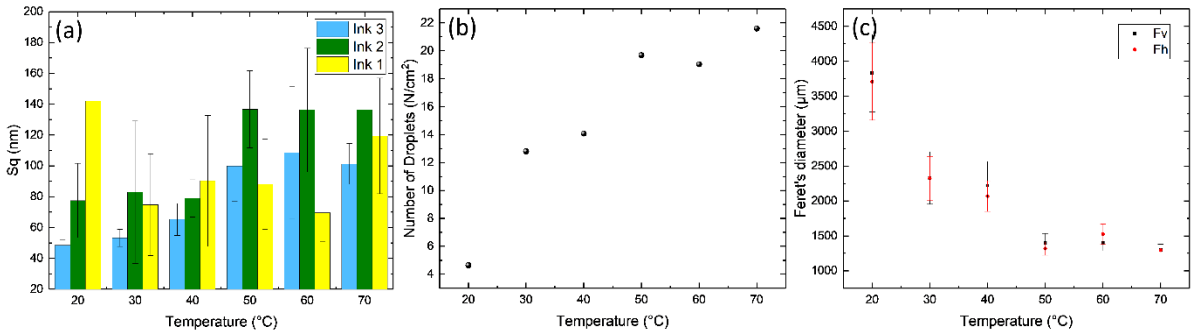

Figure S8: (a) The rms roughness (S_q) as a function of temperature. Error was calculated by standard deviation of mean (SDOM). (b) The number of droplets per unit area (N/cm^2) as a function of substrate temperature for each sprayed film in figure S6. (c) The average Feret's diameter in the horizontal (Fh) and vertical direction (Fv) as a function of substrate temperature for each sprayed film in figure S6. Error was calculated by SDOM.

1.4 Atomic force microscopy and sheet resistance of TCF films

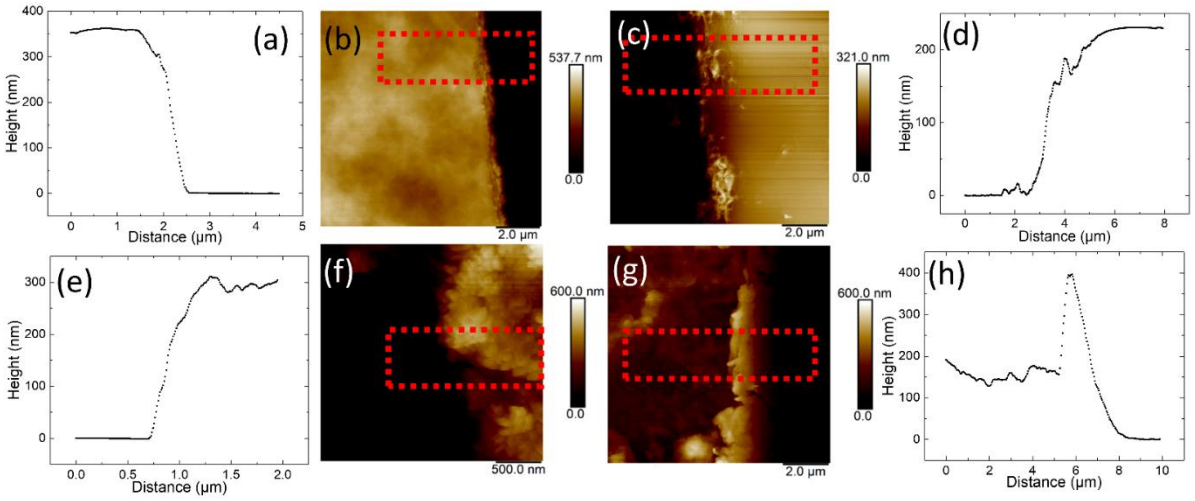

Figure S9: The spray coated average step heights of (a) PEDOT:PSS (359nm), (d) SWNT (231nm) , (e) GNP (290nm) and (h) Gr-PEDOT:PSS (156nm) are determined with AFM on Si/SiO_2 after a clean scratch was made on each film. The corresponding micrographs for (b) PEDOT:PSS-Eth, (c) SWNT-Eth, (f) GNP-Eth and (g) Gr-PEDOT:PSS-Eth are marked with a red box from which the average step height profile was taken.

Atomic force microscopy (AFM) (Bruker Dimension Icon) is used to determine the average thickness of a coating on each of the four hemispheres. Since it is difficult to characterise 3D substrates under AFM so we spray on flat Si/SiO_2 substrates ($\gamma_{SV} \approx 56$ mN/m) using the same inks and parameters which were used to spray coat the hemispheres. Figure S9 (a-h) shows AFM micrographs of the four films where the average thickness could be found for the PEDOT:PSS (359nm), SWNT (231nm), GNP (290nm) and Gr-PEDOT:PSS (156nm) films.

Subsequently sheet resistance (R_s) measurements of the GNP film (~1.2 ± 0.7 MOhm/sq), SWNT (~46 ± 1 kOhm/sq), PEDOT:PSS (~59 ± 2 Ohm/sq) and Gr-PEDOT:PSS (~640 ± 34 Ohm/sq) were undertaken on the films using a Jandel probe head in a 4-point probe configuration.

1.2 References

(1) Lotya, M.; Hernandez, Y.; King, P. J.; Smith, R. J.; Nicolosi, V.; Karlsson, L. S.; Blighe, F. M.; De, S.; Zhiming, W.; McGovern, I. T.; Duesberg, G. S.; Coleman, J. N.

Liquid Phase Production of Graphene by Exfoliation of Graphite in Surfactant/water Solutions. *J. Am. Chem. Soc.* **2009**, *131* (10), 3611–3620.

(2) Hernandez, Y.; Nicolosi, V.; Lotya, M.; Blighe, F. M.; Sun, Z.; De, S.; McGovern, I. T.; Holland, B.; Byrne, M.; Gunko, Y.; Boland, J. J.; Niraj, P.; Duesberg, G.; Krishnamurti, S.; Goodhue, R.; Hutchison, J.; Scardaci, V.; Ferrari, A. C.; Coleman, J. N.; Gun'Ko, Y. K.; Boland, J. J.; Niraj, P.; Duesberg, G.; Krishnamurthy, S.; Goodhue, R.; Hutchison, J.; Scardaci, V.; Ferrari, A. C.; Coleman, J. N. High Yield Production of Graphene by Liquid Phase Exfoliation of Graphite. *Nat. Nano.* **2008**, *3* (9), 563–568.

(3) Ferrari, A. C.; Robertson, J. Interpretation of Raman Spectra of Disordered and Amorphous Carbon. *Phys. Rev. B* **2000**, *61* (20), 14095–14107.

(4) Kouroupis-Agalou, K.; Liscio, A.; Treossi, E.; Ortolani, L.; Morandi, V.; Pugno, N. M.; Palermo, V. Fragmentation and Exfoliation of 2-Dimensional Materials: A Statistical Approach. *Nanoscale* **2014**, *6* (11), 5926–5933.

(5) Li, D.; Neumann, A. W. Equation of State for Interfacial Tensions of Solid-Liquid Systems. *Adv. Colloid Interface Sci.* **1992**, *39* (C), 299–345.

(6) Stout, K. Three Dimensional Surface Topography. *Three Dimens. Surf. Topogr.* **2000**, 19–94.

(7) Susanna, G.; Salamandra, L.; Brown, T. M.; Di Carlo, A.; Brunetti, F.; Reale, A. Airbrush Spray-Coating of Polymer Bulk-Heterojunction Solar Cells. *Sol. Energy Mater. Sol. Cells* **2011**, *95* (7), 1775–1778.

(8) Scardaci, V.; Coull, R.; Lyons, P. E.; Rickard, D.; Coleman, J. N. Spray Deposition of Highly Transparent, Low-Resistance Networks of Silver Nanowires over Large Areas. *Small* **2011**, *7* (18), 2621–2628.

(9) B. Panneton. Image Analysis of Water-Sensitive Cards for Spray Coverage

Experiments. *Appl. Eng. Agric.* **2002**, *18(2)*, 179–182.